

# A bibracchial lariat aza-crown ether as an abiotic catalyst of malonic acid enolization†

M. Paz Clares,<sup>a</sup> M. Teresa Albelda,<sup>\*a</sup> Juan Aguilar,<sup>‡\*a</sup> Luis R. Domingo,<sup>b</sup> Juan C. Frías,<sup>a</sup> Roberto Tejero,<sup>c</sup> Conxa Soriano<sup>d</sup> and Enrique García-España<sup>\*a</sup>

Received (in Durham, UK) 3rd January 2007, Accepted 13th July 2007

First published as an Advance Article on the web 6th August 2007

DOI: 10.1039/b618787k

A bibracchial lariat aza-crown ether (**L**) consisting of 2-aminoethylnaphthyl moieties appended to a 2 : 2 azapyridinophane structure displays significant activation of H–D exchange in malonic acid. The compound forms very stable adducts with malonate anions (**MA**) in the 2–10 pH range. Molecular dynamics studies performed for the species resulting from the interaction of the hexaprotonated macrocycle and the dianion show that malonate is encapsulated by **L** with distances between the CH<sub>2</sub> group of malonate and the pyridine nitrogens of *ca.* 3.5 Å. The pendant arms of **L** cap above and below the anion, defining a pseudo-cage structure. Quantum chemical calculations for  $\alpha$ -proton abstraction from malonate by the protonated ligand **L**, at the B3LYP/6-31G\*\* computational level using reduced models, have allowed transition states to be obtained that denote a concerted mechanism in which  $\alpha$ -proton abstraction is accompanied by proton transfer from protonated amino groups of the receptor to the carboxylate groups. Kinetic measurements for ligand **L**, performed at pD = 6 following the variation of the <sup>1</sup>H-NMR **MA**-CH<sub>2</sub> and **MA**-CHD signals, allow the following rate constants to be calculated:  $k_1^H = (60.2 \pm 0.5) \times 10^{-3} \text{ min}^{-1}$  and  $k_2^H = (75.3 \pm 0.6) \times 10^{-3} \text{ min}^{-1}$ , with values that equal the experimental values of the free substrate at pD = 0. The rate enhancement produced by the open-chain reference ligand (**L**<sub>1</sub>), containing the polyamine tren (tris(2-aminoethyl)amine) functionalized at one of its terminal amino groups with a naphthyl moiety, is much more moderate, with  $k_1^H = (9.2 \pm 0.2) \times 10^{-3} \text{ min}^{-1}$  and  $k_2^H = (11.56 \pm 0.03) \times 10^{-3} \text{ min}^{-1}$ .

## Introduction

Nature has a unique approach to generating a huge variety of products.<sup>1</sup> The biosynthesis of these compounds is often accomplished by multi-domain proteins with remarkable architectures and multi-enzyme pathways that comprise the synthetic machinery of biological systems.<sup>2</sup> Mimicking enzymes using artificial entities has been the impetus for many research groups over the past 20 years and the design and synthesis of artificial receptors for selective recognition of bioactive substrates have received considerable interest.<sup>3</sup>

Many enzymes are members of families that catalyze reactions in the chemistry of life, transforming both macromolecular substrates and small molecules.<sup>2,4</sup> Enolase is an enzyme present in muscle tissues that participates in glycolysis and acts in carbohydrate metabolism. Enolase is a homodimer metal-activated metalloenzyme which uses two magnesium ions per subunit: the strongly bound conformational ion and the catalytic one that binds to the enzyme–substrate complex inducing the catalysis process that consists of the abstraction of a proton from a carbon atom adjacent to a carbonyl/carboxylic group ( $\alpha$ -proton of a carbon acid).<sup>5</sup>

In recent years, several receptors have been evaluated as enolase mimics. Breslow and co-workers<sup>6</sup> have pioneered the field using modified  $\beta$ -cyclodextrins and more recently Menger and Binder<sup>7</sup> have explored the possibilities of an amino derivative of this type of compound. Although  $\beta$ -cyclodextrins were the first examples of abiotic catalysts for enolization in water, other macrocycles and molecules were examined that showed an improvement in catalytic efficiency.<sup>8</sup> Lehn *et al.*<sup>8</sup> have employed aza-crowns to catalyze H–D exchange using malonate as a substrate. Polyammonium macrocycles combine several properties that make them potentially suitable as general acid–base catalysts (Scheme 1).

Here we report on a synthetic receptor (**L**) with promising features for supramolecular electrophilic catalysis in the activation of  $\alpha$ -proton exchange.

<sup>a</sup> Departamento de Química Inorgánica, Instituto de Ciencia Molecular (ICMOL), Universidad de Valencia, Edificio de Institutos de Paterna, Apartado de Correos 22085, 46071 Valencia, Spain.

E-mail: teresa.albelda@uv.es. E-mail: juan.aguilar@uv.es. E-mail: enrique.garcia-es@uv.es; Tel: (+34) 963544879

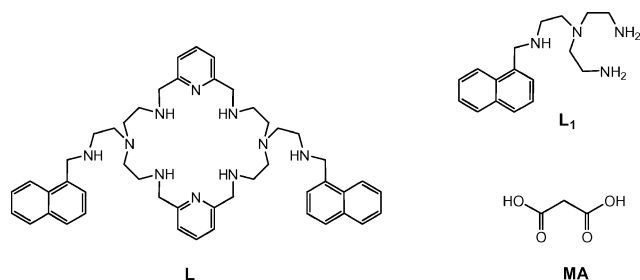
<sup>b</sup> Departamento de Química Orgánica, Facultad de Químicas, Universidad de Valencia, Edificio Jeroni Muñoz, 46100 Burjassot Valencia, Spain

<sup>c</sup> Departamento de Química Física, Facultad de Químicas, Universidad de Valencia, Edificio Jeroni Muñoz, 46100 Burjassot Valencia, Spain

<sup>d</sup> Departamento de Química Orgánica, Instituto de Ciencia Molecular (ICMOL), Universidad de Valencia, Edificio de Institutos de Paterna, Apartado de Correos 22085, 46071 Valencia, Spain

† Electronic supplementary information (ESI) available: Speciation diagram for **L** with malonic acid, <sup>1</sup>H NMR data and calculated rate constants for H–D exchange. See DOI: 10.1039/b618787k.

‡ Current address: Department of Chemistry, University of York, Heslington, York, UK, YO10 5DD.



Scheme 1 Ligands **L** and **L**<sub>1</sub> and malonic acid (**MA**).

## Results and discussion

One approach to the design of artificial enolases consists of the construction of a receptor with a pre-designed topology that includes: a semi-rigid macrocycle scaffold able to strongly bind the acidic and basic forms of the substrate; some type of electrophilic catalyst such as a metal-ion, charge pairing, or hydrogen bonding interactions in order to increase the acidity of the substrate; and the incorporation of a hydrophobic environment surrounding the region of electrophilic interaction. Receptor **L** possesses a cyclic core with the ability to carry a high positive charge through protonation whilst presenting unprotonated nucleophilic sites at the same time. It has been reported that this bibracchial lariat aza-crown ligand forms stable complexes with aliphatic carboxylic acids that are suitable substrates for  $\alpha$ -proton abstraction.<sup>9</sup> Additionally, **L** possesses two arms with naphthalene units that allow the molecule to adopt different conformations as previously reported.<sup>10</sup> In one of these conformers, the aromatic moieties are placed at the top and the bottom of the macrocyclic cavity.

### Binding studies

The determination of the host–guest interaction constants was performed using potentiometric techniques. Table 1 shows the stability constants for the interaction of receptor **L** with malonic acid and Fig. S1 (ESI<sup>†</sup>) displays the speciation diagram for this system.

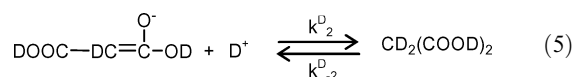
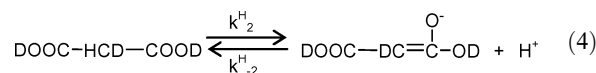
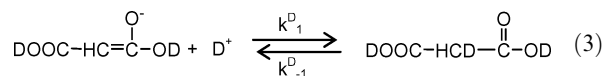
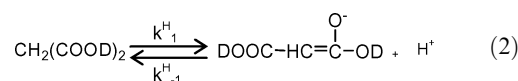
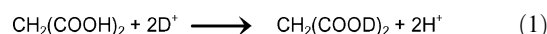
An examination of Table 1 and Fig. S1<sup>†</sup> shows that protonated receptor **L** binds malonate ions and forms stable complexes in the 2–10 pH range. At low pH (<2), malonate ions are protonated<sup>11</sup> and there is no evidence of interaction with the protonated ligand; at high pH (>10), the macrocycle is unprotonated and does not bind malonate ions; at pH  $\approx$  6.5, receptor **L** can interact with dianionic malonate, allowing the formation of tri-, tetra-, penta- and hexaprotonated com-

plexes. Therefore, receptor **L** is a good candidate for investigating the effect of binding on the H–D exchange in malonate ions.

### Kinetics of exchange

The kinetics of deuteration for the systems **MA**, **L**–**MA** and **L**<sub>1</sub>–**MA** were determined by <sup>1</sup>H NMR spectroscopy at pD = 6. Fig. 1 shows <sup>1</sup>H-NMR spectra at pD = 6 for malonic acid in the course of the H–D exchange. The singlet corresponds to the **MA**-CH<sub>2</sub> protons, while the triplet is attributed to the **MA**-CHD proton (the multiplicity is due to a proton–deuterium coupling constant). Kinetic rate constants could be determined by following the triplet and the singlet intensities in <sup>1</sup>H-NMR experiments recorded at different times.

Hansen and Ruoff<sup>12</sup> proposed a mechanism for isotopic-exchange reactions occurring when malonic acid or 2-substituted malonic acids are dissolved in D<sub>2</sub>SO<sub>4</sub>. The deuteration reaction starts with a very rapid exchange of the carboxylic protons by D<sup>+</sup> (1) and then this is followed by a sequence in which the enol form of malonic acid acts as an intermediate (2–5).



Hansen and Ruoff<sup>12</sup> demonstrated that, although all steps are potentially reversible, reactions (2) and (4) were practically irreversible under the reaction conditions because any H<sup>+</sup> formed was rapidly absorbed in the 1 M D<sub>2</sub>SO<sub>4</sub>–D<sub>2</sub>O medium. We have studied the interaction of receptors **L** and **L**<sub>1</sub> with malonic acid at pD = 6 and in both cases catalyzed isotope exchange reactions were observed. Peak height measurements have been used for quantification instead of peak area due to the overlapping of the signals.

Table 2 summarizes the enolization rate constants calculated according to ref. 12. It is interesting to note that the

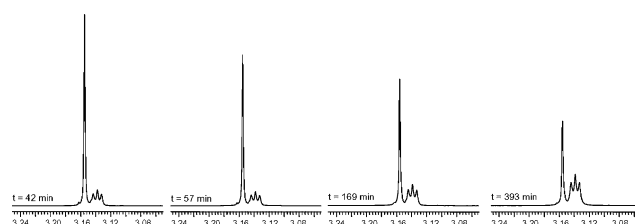


Fig. 1 <sup>1</sup>H-NMR spectra at different times for malonic acid at pD = 6 showing the variation of the singlet (**MA**-CH<sub>2</sub>) and triplet (**MA**-CHD proton) peaks.

Table 1 Selected stepwise logarithms of the stability constants (log *K*) for the interaction of **L** with malonic acid determined in 0.15 mol dm<sup>−3</sup> NaCl at *T* = 298.1 K

Reaction <sup>a</sup>	log <i>K</i>
LH + A ⇌ LAH	4.83 ± 0.03
LH <sub>2</sub> + A ⇌ LAH <sub>2</sub>	5.67 ± 0.03
LH <sub>3</sub> + A ⇌ LAH <sub>3</sub>	6.27 ± 0.03
LH <sub>4</sub> + A ⇌ LAH <sub>4</sub>	6.24 ± 0.03
LH <sub>5</sub> + A ⇌ LAH <sub>5</sub>	6.70 ± 0.03
LH <sub>6</sub> + A ⇌ LAH <sub>6</sub>	6.59 ± 0.06
LH <sub>6</sub> + AH ⇌ LAH <sub>7</sub>	6.36 ± 0.03

<sup>a</sup> Charges omitted for clarity.

**Table 2** Calculated rate constants ( $\text{min}^{-1}$ ) for the H–D exchange reaction of the  $\alpha\text{-CH}_2$  of malonic acid catalyzed by sulfuric acid and studied polyamine receptors

	Values $\times 10^3/\text{min}^{-1}$			
	MA ( $\text{D}_2\text{SO}_4$ 1 M) <sup>a</sup>	MA (pD = 6)	L–MA (pD = 6)	L <sub>1</sub> –MA (pD = 6)
$k_1^{\text{H}}$	64.02(2) <sup>b</sup>	3.74(3)	60.2(5)	9.2(2)
$k_2^{\text{H}}$	25(1)	2.4(1)	75.3(6)	11.56(3)

<sup>a</sup> Obtained from ref. 12. <sup>b</sup> Values in parenthesis are standard deviations in the last significant figure.

macrocyclic polyamine **L** gives the same enhancement rate as that obtained for the free substrate in 1 M  $\text{D}_2\text{SO}_4$ . As can be seen in Fig. 2, where the normalized peak intensities obtained for the MA–CHD signal are plotted against reaction time for each of the studied systems, receptor **L** is much more efficient than **L**<sub>1</sub> in terms of catalysis.

The variation in the rate constant values obtained for **L** and **L**<sub>1</sub> can be attributed to two main differences between these two ligands, namely: the presence or absence of the pyridine group and the topological factor (*i.e.*, the different shape and flexibility of each receptor). Both the topology and the presence of the pyridine group could play an important role in facilitating the  $\alpha$ -proton abstraction, since a pyridine group placed at the right distance could act as a general base. This assumption is further supported by the theoretical studies (*vide infra*) and the NMR data. Fig. 3 shows the time-evolution for the **L**–MA system. Broad pyridine signals centered at 7.4 and 7.9 ppm were resolved after addition of malonic acid to the ligand. This fact might indicate a conformational change induced by the malonic acid and points out the involvement of the pyridine unit in the reaction mechanism (see section on molecular mechanics studies). In the aliphatic area, the peak at 4.3 ppm, attributed to one of the methylene protons closer to the pyridine ring, becomes well-resolved and sharper with malonic acid interaction, indicating a conformational change has taken place in that part of the molecule.

Although calculated kinetic data for our systems fit properly with the irreversible mathematical models proposed by Hansen and Ruoff,<sup>12</sup> evidence of reversibility was detected. After two weeks of reaction, the CHD triplet in  $^1\text{H}$ -NMR

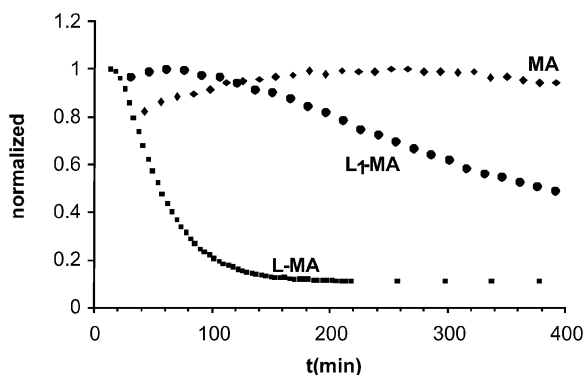


**Fig. 2** Plot of the normalized intensities of –CHD– peaks of malonic acid (MA), **L**–MA and **L**<sub>1</sub>–MA vs. reaction time at pD = 6.

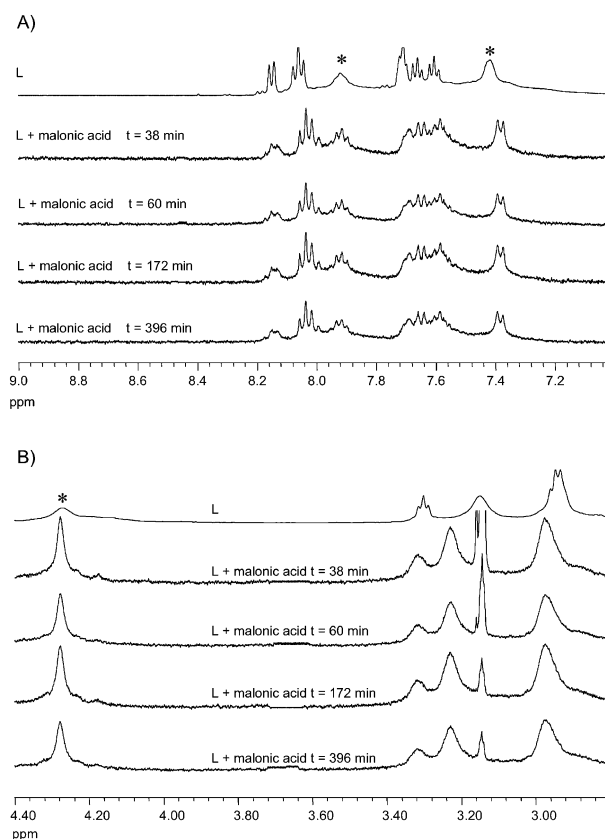


**Fig. 3**  $^1\text{H}$  NMR spectra for the system **L**–MA registered at pD = 6; (A) aromatic and (B) aliphatic regions of the spectra. The first spectrum in each series corresponds to macrocycle **L**. Peaks labelled with \* are resolved after addition of MA.

spectrum of the **L**–MA system is still observable, confirming that the two central hydrogen atoms of malonic acid have not been replaced completely by deuterium and therefore the reversibility of the reaction. Although the samples were prepared under argon using 99.9% deuterated water, the residual triplet could be attributed to the presence of some  $\text{H}_2\text{O}$  arising from hydration of polyamines, water from  $\text{D}_2\text{O}$  or hydration of the samples while experiments were recorded. However, the system can be treated essentially as non-reversible.

Even though it is difficult to establish comparisons between the values reported in the literature due to the differences in conditions and parameters, calculated rate constants of macrocycle **L** for H–D exchange reaction are in the same range as those calculated for [24]ane $\text{N}_4\text{O}_2$ ,<sup>8</sup> cyclen derivatives<sup>13</sup> or cyclodextrins;<sup>6,7</sup> only receptor [36]ane $\text{N}_8\text{O}_4$ <sup>8</sup> seems to be a more efficient catalyst for  $\alpha$ -proton abstraction (Table S1†).

### Molecular mechanics and dynamic studies

Fig. 4 shows a superposition of ten models with the lowest energies extracted from the trajectories of molecular dynamics simulations (part A) and the minimum energy model (part B). The superposition has been made taking the malonic atoms as a reference. The minimum energy models locate malonic acid right in the core of the macrocycle **L** and parallel to the pyridine rings. The nitrogens of the cyclic frame stabilize

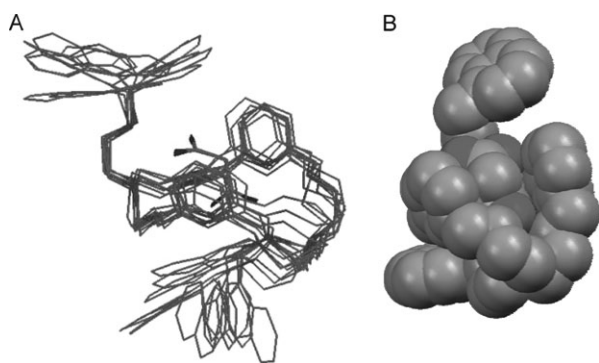
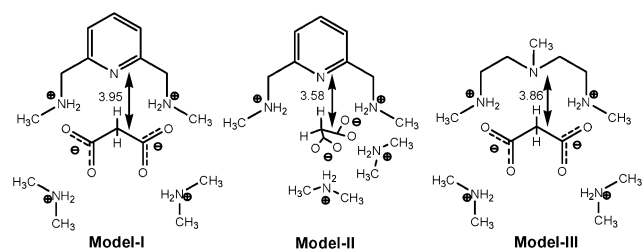


**Fig. 4** Superposition of the ten minimum energy models from molecular dynamics simulations (A) taking malonic atoms as a reference and minimum energy model (B) for the system **L-MA**.

carboxylate groups and the distance between the central  $-\text{CH}_2-$  and the pyridine nitrogens is short enough (3.5 and 4.1 Å) to enable the aromatic ring to behave as a base and remove the acidic protons. This location of malonic acid can justify the sharpening of the  $^1\text{H}$  NMR benzylic and pyridine aromatic signals. Each of the carboxylate rings is interacting with three secondary amino groups, two from the macrocyclic framework and one from the pendant arms; the O–N distances are in the range 2.7–3.2 Å suggesting the possibility of formation of a hydrogen bonding network that would contribute to stabilizing the adduct species.

#### Quantum chemical calculations for $\alpha$ -proton abstraction from malonate by the protonated ligand **L**

In order to gain insight into the possible mechanism and transition state for the H–D exchange process, we have carried out a quantum chemical study of the transition state structures involved in the  $\alpha$ -proton abstraction from malonate at the B3LYP/6-31G\*\* computational level. Due to the large number of atoms present in **L**, three reduced models containing relevant features of ligand **L** provided by the molecular mechanics and dynamics study were considered (Scheme 2). In model I and model II, the nitrogen atom of the pyridine moiety was chosen as the proton acceptor, while in model III, the selected proton acceptor was the nitrogen atom of one of the tertiary amines present in **L**. In model I the malonate is extended parallel to the pyridine plane containing the 2,6-substituents, while in model II, the dianion is normal to the pyridine ring. This last situation will somehow agree with the relative dispositions obtained in the minimum energy ground state conformers obtained in the molecular dynamics studies (Fig. 4). These minimum energy conformers, along



**Scheme 2** Models used in computational studies.

with the NMR data, somewhat support the participation of pyridine as the base in  $\alpha$ -proton abstraction. On the other hand, these three moieties are repeated several times within the molecular structure of **L**. The models are completed by two protonated secondary amino groups linked to the acceptor atom through methylene groups and by two dimethylammonium moieties that have been included in order to model the other ammonium groups present in cyclic framework (models I and III) or in the pendant arm (model II) of **L** (Scheme 2). Indeed, it has been shown that the rate enhancements provided by structures like diethylenetriamine<sup>8</sup> or **L**<sub>1</sub> itself are very modest and therefore additional charged sites are required to operate the concerted  $\alpha$ -proton abstraction mechanism (*vide infra*). In these computational models, the incorporated malonate anion presents a near-planar conformation in which the four oxygen atoms are hydrogen-bonded to the four ammonium cations.

Full geometrical optimization of the corresponding precursor complexes gives three structures in which the average distance between the four oxygen atoms of malonate and the hydrogen atoms of the protonated amino groups is *ca.* 1.50 Å. The distances between the methylene carbon of malonate and the pyridine and tertiary amine nitrogen atoms are 3.95, 3.58 and 3.86 Å, respectively.

A search for the transition state structures associated with proton abstraction in **L** provided structures **TS-I**, **TS-II** and **TS-III** for models I, II and III, respectively (Fig. 5). **TS-I** presents higher molecular symmetry than **TS-II**, but the latter shows an 8.5 kcal mol<sup>−1</sup> lower energy. In these transition state structures, the two added dimethylammonium groups remain at the same relative positions as in the precursor complexes. In all TSs, the distances between the donor methylene carbon and the acceptor nitrogens are reduced to 2.8 Å. The distances of the abstracted proton to the carbon donor and the nitrogen acceptors are 1.57 and 1.24 Å in **TS-I**, 1.59 and 1.20 Å in **TS-II** and 1.51 and 1.27 Å in **TS-III**, respectively. It is interesting to emphasize that in the three transition states, there is a concerted proton transfer from the ammonium residues neighbouring the proton acceptor nitrogens to the carboxylate groups. This would allow the high negative charge developed

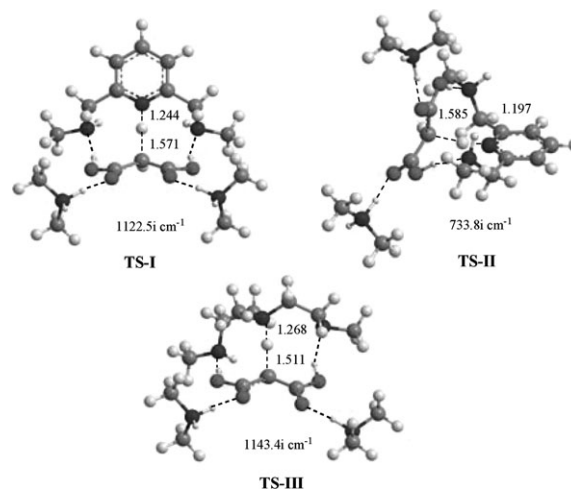


**Fig. 5** Proposed transition state structures.



on the substrate following the formation of the corresponding enolates to be reduced. It is known that electrophilic catalysis can induce a decrease of the  $pK_a$  of the  $\alpha$ -CH by up to 15 units upon protonation of the carboxylic group.<sup>14</sup>

Once the enolate is formed, the  $\alpha$ -proton is completely transferred to the acceptor nitrogens, the distance between the abstracted proton and the carbon atom of enolate becoming 2.12 Å. The enolates present in both TSs have a planar conformation with C–C bond lengths of 1.43 Å.

## Conclusions

The activities of **L** and **L**<sub>1</sub> as catalysts for proton exchange have been investigated. The studies demonstrate the ability of these receptors to bind malonate anions and catalyze H–D exchange at the –CH<sub>2</sub>– position. In particular, macrocycle **L** ranks amongst the synthetic receptors yielding the largest rate acceleration of the process. Moieties formed by a non-protonated amino group with two neighbouring ammonium groups seem to match perfectly the size and disposition of malonate anion allowing the concerted mechanism of  $\alpha$ -proton exchange. However, additional protonated sites able to neutralize the high negative charge developed in the enolization process are also important requisites.

## Experimental

The syntheses of **L** and **L**<sub>1</sub> have been reported elsewhere.<sup>10</sup>

### Electromotive force measurements

The potentiometric titrations were carried out at  $298.1 \pm 0.1$  K using NaCl 0.15 mol dm<sup>−3</sup> as supporting electrolyte. The experimental procedure (burette, potentiometer, cell, stirrer, microcomputer, *etc.*) has been fully described elsewhere.<sup>15</sup> The acquisition of the emf data was performed with the computer program PASAT.<sup>16</sup> The reference electrode was an Ag/AgCl electrode in saturated KCl solution. The glass electrode was calibrated as a hydrogen-ion concentration probe by titration of previously standardized amounts of HCl with CO-free NaOH solutions and determining the equivalent point by the Gran method,<sup>17</sup> which gives the standard potential,  $E^\circ$ , and the ionic product of water ( $pK_w = 13.73(1)$ ).

The computer program HYPERQUAD<sup>18</sup> was used to calculate the protonation and stability constants. The pH range investigated was 2.0–11.0. The different titration curves for each ligand were treated as separated curves without significant variations in the values of the stability constants. Finally, the sets of data were merged together and treated simultaneously to give the final stability constants.

### NMR sample preparation

NMR samples were prepared under an argon atmosphere at  $pD = 6$  in D<sub>2</sub>O (Aldrich, 99.9%). Adjustments to the desired  $pD$  were made using drops of DCl or NaOD solutions. Values of  $pD$  are given without correction.<sup>19</sup>  $[L] = [L_1] = 0.02$  M,  $[MA] = 0.2$  M.

### NMR acquisition and processing parameters

The NMR spectra were recorded using either a Bruker Avance 400 (400 MHz, 100 MHz) or a Bruker Avance DPX-500 (500 MHz, 125 MHz) NMR spectrometer. Spectra were obtained using a 5 mm inverse broadband probe head incorporating a shielded Z-gradient coil. Typically, a sample was tested over a period of 800 min, recording <sup>1</sup>H NMR experiments every 14 min using a 30° pulse angle and a 1.0 s relaxation delay. Each experiment consisted of 10 scans, taking 12 s per experiment. Experiments were performed directly in the spectrometer at  $25.0 \pm 0.2$  °C and there was a time delay of approximately 15–30 min between mixing of the reagents, adjusting the  $pD$  and the start of NMR measurements, resulting from inserting the tube into the instrument and fine shimming (*i.e.* improving the magnetic field homogeneity) of the sample. Although, during these 15–30 min, the concentration of non-deuterated water may have increased by up to 1%, there was no difficulty in extrapolating the data to the initial conditions ( $t = 0$ ).

All chemicals were of analytical grade and were used without further purification.

### Molecular dynamics simulations

Molecular dynamics simulations were carried out using AMBER8<sup>20</sup> and GAFF potentials<sup>21</sup> at 325 K. The process comprised a convenient heating stage (in several steps until a final temperature of 325 K was reached) after which the simulation was done. The heating stage comprised 6 steps along which the temperature was slowly increased for a period of 30 ps plus 2 steps, of 20 ps each, at the end until the target temperature was reached, namely 325 K. Then the system was ready for a production stage of 77 ns, along which energies and data were saved every 500 steps (each step 0.2 fs). Minimum energy conformers were extracted from the trajectories and are given in Fig. 4 (part A) of the manuscript. The calculations were performed for the interaction of the hexa-protonated macrocycle with malonate dianion. The protons are located in the secondary amino groups of the receptor. Files with trajectories in AMBER8<sup>20</sup> format and GAFF potentials<sup>21</sup> at 325 K are available on request.

### Quantum chemical calculations

Density functional theory (DFT) calculations have been carried out using the B3LYP<sup>22</sup> exchange–correlation functionals, together with the standard 6-31G\*\* basis sets.<sup>23</sup> The optimizations were carried out using the Berny analytical gradient optimization method.<sup>24</sup> All calculations were carried out with the Gaussian 03 suite of programs.<sup>25</sup>

## Acknowledgements

Financial support from the DGICYT project CTQ2006-15672-CO5-01, FEDER-assisted, is gratefully acknowledged. One of us, MTA, wants to thank Ministerio de Educación y Ciencia of Spain for a Juan de la Cierva contract.

## References

- (a) P. Ball, *Nat. Mater.*, 2003, **2**, 510; (b) P. Ball, *Nanotechnology*, 2002, **13**, R15.

- 2 J. M. Berg, L. Stryer and J. L. Tymoczko, *Biochemistry*, W. H. Freeman, New York, 5th edn, 2002; R. H. Garrett and C. M. Grisham, *Principles of Biochemistry With a Human Focus*, Brooks/Cole, Belmont, USA, 2001; D. L. Nelson and M. M. Cox, *Lehninger Principles of Biochemistry*, W. H. Freeman, New York, 4th edn, 2005.
- 3 (a) V. Amendola, M. Bonizzoni, D. Esteban-Gómez, L. Fabbrizzi, M. Licchelli, F. Sancenón and A. Taglietti, *Coord. Chem. Rev.*, 2006, **250**, 1451; (b) I. Iranza, Y. A. Kovalevsky, J. R. Morrow and J. P. Richard, *J. Am. Chem. Soc.*, 2003, **125**, 1988; (c) M.-Y. Yang, J. P. Richard and J. R. Morrow, *Chem. Commun.*, 2003, 2832; (d) H. Sakiyama, Y. Igarashi, Y. Nakayama, M. J. Hossain, K. Unoura and Y. Nishida, *Inorg. Chim. Acta*, 2003, **351**, 256; (e) J. Gong and B. C. Gibb, *Org. Lett.*, 2004, **6**, 1353; (f) R. Breslow and S. D. Dong, *Chem. Rev.*, 1998, **98**, 1997; (g) N. V. Kaminskaia, B. Spingler and S. J. Lippard, *J. Am. Chem. Soc.*, 2001, **123**, 6555; (h) Y. Kim, J. T. Welch, K. M. Lindstrom and S. J. Franklin, *JBC*, *J. Biol. Inorg. Chem.*, 2001, **6**, 173; (i) S. L. Tobey and E. V. Anslyn, *J. Am. Chem. Soc.*, 2003, **125**, 10963.
- 4 C. Walsh, *Nature*, 2001, **409**, 226.
- 5 (a) O. Warburg and W. Christian, *Biochem. Z.*, 1941, **310**, 384; (b) L. Lebiada, B. Stec and J. M. Brewer, *J. Biol. Chem.*, 1989, **264**, 3685; (c) J. E. Wedekind, R. R. Poyner, G. H. Reed and I. Rayment, *Biochemistry*, 1994, **33**, 9333; (d) T. M. Larsen, J. E. Wedekind, I. Rayment and G. H. Reed, *Biochemistry*, 1996, **35**, 4349.
- 6 (a) B. Siegel, A. Pinter and R. Breslow, *J. Am. Chem. Soc.*, 1977, **99**, 2309; (b) R. Breslow and A. Graf, *J. Am. Chem. Soc.*, 1993, **115**, 10988; (c) J. M. Desper and R. Breslow, *J. Am. Chem. Soc.*, 1994, **116**, 12081; (d) R. Breslow, J. M. Desper and Y. Huang, *Tetrahedron Lett.*, 1996, **37**, 2541.
- 7 W. H. Binder and F. M. Menger, *Tetrahedron Lett.*, 1996, **37**, 8963.
- 8 (a) J. Wolfe, A. Muehldorf and J. Rebek, Jr, *J. Am. Chem. Soc.*, 1991, **113**, 1453; (b) H. Fenniri, J.-M. Lehn and A. Marquis-Rigault, *Angew. Chem., Int. Ed. Engl.*, 1996, **35**, 337; (c) T. Chin, Z. N. Gao, I. Lelouche, Y. G. K. Shin, A. Purandare, S. Knapp and S. S. Isied, *J. Am. Chem. Soc.*, 1997, **119**, 12849; (d) E. Kimura, H. Kitamura, T. Koike and M. Shiro, *J. Am. Chem. Soc.*, 1997, **119**, 10909; (e) A. M. Kelly-Rowley, V. M. Lynch and E. V. Anslyn, *J. Am. Chem. Soc.*, 1995, **117**, 3438; (f) T. S. Snowden, A. P. Bisson and E. V. Anslyn, *Bioorg. Med. Chem.*, 2001, **9**, 2467.
- 9 M. P. Clares, C. Lodeiro, D. Fernández, A. J. Parola, F. Pina, E. García-España, C. Soriano and R. Tejero, *Chem. Commun.*, 2006, 3824.
- 10 M. P. Clares, J. Aguilar, R. Aucejo, C. Lodeiro, M. T. Albelda, F. Pina, J. C. Lima, A. J. Parola, J. Pina, J. Seixas de Melo, C. Soriano and E. García-España, *Inorg. Chem.*, 2004, **43**, 6114.
- 11 Ionization constants:  $pK_a = 2.63$  and  $5.27$ : R. J. Motekaitis and A. E. Martell, *Inorg. Chem.*, 1992, **31**, 5534.
- 12 E. W. Hansen and P. Ruoff, *J. Phys. Chem.*, 1988, **92**, 2641.
- 13 E. Kimura, T. Gotoh, T. Koike and M. Shiro, *J. Am. Chem. Soc.*, 1999, **121**, 1267.
- 14 (a) J. A. Gerlt and P. G. Gassman, *J. Am. Chem. Soc.*, 1992, **114**, 5928; (b) Y. Chiang and A. J. Kresge, *Science*, 1991, **253**, 395.
- 15 E. García-España, M. J. Ballester, F. Lloret, J.-M. Moratal, J. Faus and A. Bianchi, *J. Chem. Soc., Dalton Trans.*, 1988, 101.
- 16 M. Fontanelli and M. Micheloni, *Proceedings of the I Spanish-Italian Congress on Thermodynamics of Metal Complexes*, Diputación de Castellón, Castellón, Spain, 1990.
- 17 (a) G. Gran, *Analyst*, 1952, **77**, 661; (b) F. J. C. Rossotti and H. Rossotti, *J. Chem. Educ.*, 1965, **42**, 375.
- 18 P. Gans, A. Sabatini and A. Vacca, *HypNMR2000*, version 2.0(NT), Protonic Software, 1999 (peter.gans@hyperquad.co.uk).
- 19 A. K. Covington, M. Paabo, R. A. Robinson and R. G. Bates, *Anal. Chem.*, 1968, **40**, 700.
- 20 D. A. Case, T. A. Darden, T. E. Cheatham, III, C. L. Simmerling, J. Wang, R. E. Duke, R. Luo, K. M. Merz, B. Wang, D. A. Pearlman, M. Crowley, S. Brozell, V. Tsui, H. Gohlke, J. Mongan, V. Hornak, G. Cui, P. Beroza, C. Schafmeister, J. W. Caldwell, W. S. Ross and P. A. Kollman, *AMBER 8*, University of California, San Francisco, 2004.
- 21 J. M. Wang, R. M. Wolf, J. W. Caldwell, P. A. Kollman and D. A. Case, *J. Comput. Chem.*, 2004, **25**, 1157.
- 22 (a) A. D. Becke, *J. Chem. Phys.*, 1993, **98**, 5648–5652; (b) C. Lee, W. Yang and R. G. Parr, *Phys. Rev. B: Condens. Matter Mater. Phys.*, 1988, **37**, 785.
- 23 W. J. Hehre, L. Radom, P. v. R. Schleyer and J. A. Pople, *Ab initio Molecular Orbital Theory*, Wiley, New York, 1986.
- 24 (a) H. B. Schlegel, *J. Comput. Chem.*, 1982, **3**, 214; (b) H. B. Schlegel, *Geometry Optimization on Potential Energy Surfaces, in Modern Electronic Structure Theory*, ed. D. R. Yarkony, World Scientific Publishing, Singapore, 1995, pp. 459–500.
- 25 M. J. Frisch, G. W. Trucks, H. B. Schlegel, G. E. Scuseria, M. A. Robb, J. R. Cheeseman, J. A. Montgomery, Jr., T. Vreven, K. N. Kudin, J. C. Burant, J. M. Millam, S. S. Iyengar, J. Tomasi, V. Barone, B. Mennucci, M. Cossi, G. Scalmani, N. Rega, G. A. Petersson, H. Nakatsuji, M. Hada, M. Ehara, K. Toyota, R. Fukuda, J. Hasegawa, M. Ishida, T. Nakajima, Y. Honda, O. Kitao, H. Nakai, M. Klene, X. Li, J. E. Knox, H. P. Hratchian, J. B. Cross, V. Bakken, C. Adamo, J. Jaramillo, R. Gomperts, R. E. Stratmann, O. Yazyev, A. J. Austin, R. Cammi, C. Pomelli, J. Ochterski, P. Y. Ayala, K. Morokuma, G. A. Voth, P. Salvador, J. J. Dannenberg, V. G. Zakrzewski, S. Dapprich, A. D. Daniels, M. C. Strain, O. Farkas, D. K. Malick, A. D. Rabuck, K. Raghavachari, J. B. Foresman, J. V. Ortiz, Q. Cui, A. G. Baboul, S. Clifford, J. Cioslowski, B. B. Stefanov, G. Liu, A. Liashenko, P. Piskorz, I. Komaromi, R. L. Martin, D. J. Fox, T. Keith, M. A. Al-Laham, C. Y. Peng, A. Nanayakkara, M. Challacombe, P. M. W. Gill, B. G. Johnson, W. Chen, M. W. Wong, C. Gonzalez and J. A. Pople, *GAUSSIAN 03 (Revision C.02)*, Gaussian, Inc., Wallingford, CT, 2004.